Kenific et al., http://www.jcb.org/cgi/content/full/jcb.201503075/DC1

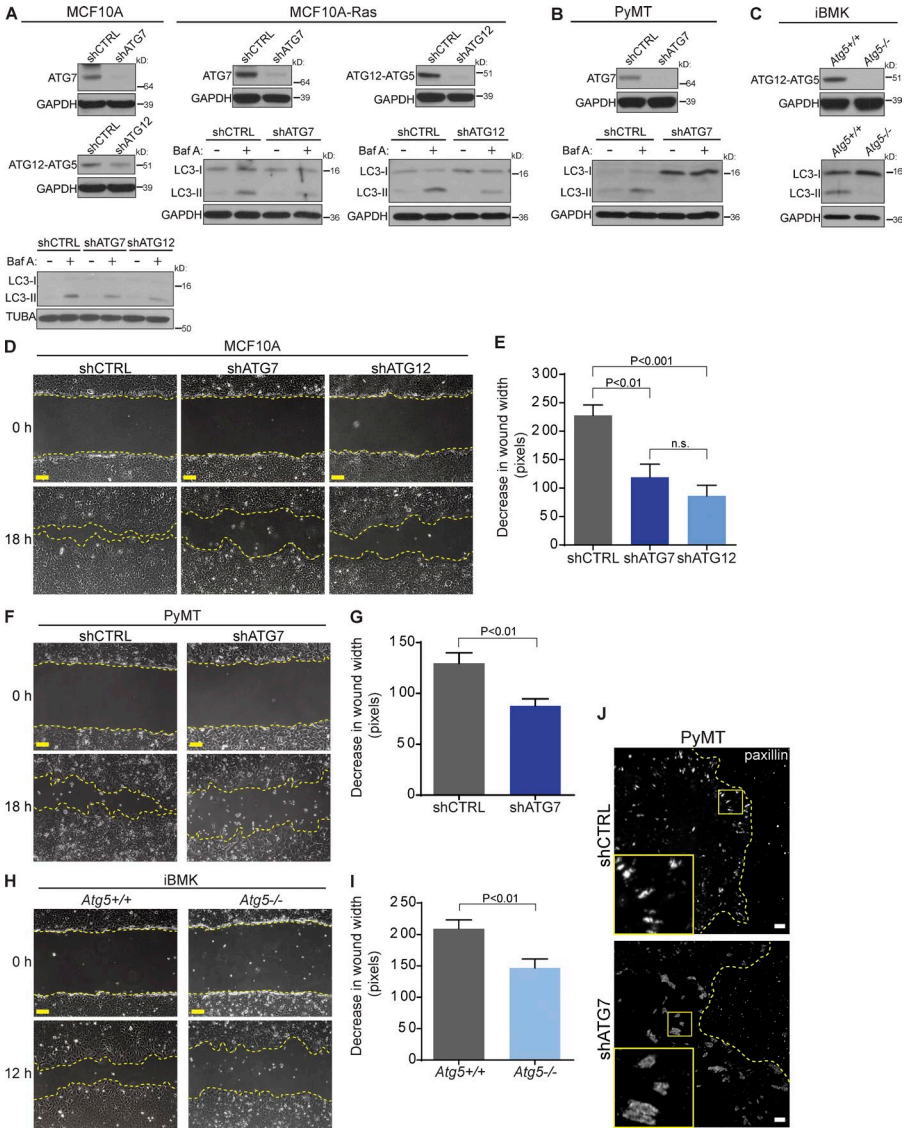

Figure S1. **Autophagy enables migration of multiple cell types.** (A) Stable shRNA-mediated depletion of ATG7 or ATG12 inhibits autophagy in wild-type MCF10A (left) and MCF10A-Ras (right) cells. ATG12 knockdown results in decrease of the ATG12-ATG5 complex required for autophagosome formation. Autophagy inhibition in ATG7- or ATG12-depleted cells shown by reduced LC3-II turnover in the presence versus absence of the lysosomal inhibitor bafilomycin A (Baf A, 20 nM for 30 min). GAPDH or α-tubulin used as loading control. (B) shRNA-mediated depletion of ATG7 inhibits autophagy in PyMT cells. LC3-II turnover was assessed as in A. GAPDH is the loading control. (C) Absence of ATG12-ATG5 and loss of autophagy (LC3-II) in iBMK cells derived from *Atg5*$^{-/-}$ mice but not *Atg5*$^{+/+}$ controls. GAPDH used as loading control. (D) Representative phase-contrast microscopy images of MCF10A cells expressing indicated shRNAs at time of wounding (0 h) and at 18 h. Dashed yellow lines highlight wound boundaries. Bars, 100 µm. (E) Quantification of wound closure over 18 h for MCF10A cells. Decrease in wound width determined by subtracting the final width at 18 h from the initial width at 0 h. Bar graph shows mean + SEM, representing $n = 12$ wounds for shCTRL, $n = 12$ wounds for shATG7, and $n = 8$ wounds for shATG12 pooled from six independent experiments. P-values determined using a one-way analysis of variance followed by Tukey post-hoc test. n.s., not significant. (F) Representative phase-contrast microscopy images of PyMT cells expressing shCTRL or shATG7 at time of wounding (0 h) and 18 h. Dashed yellow lines highlight wound boundaries. Bars, 100 µm. (G) Quantification of wound closure over 18 h for PyMT cells. Bar graph shows mean + SEM, representing $n = 16$ wounds for shCTRL and $n = 20$ wounds for shATG7 pooled from eight independent experiments. P-value determined using unpaired *t* test. (H) Representative phase-contrast microscopy images of *Atg5*$^{+/+}$ and *Atg5*$^{-/-}$ iBMK cells at time of wounding (0 h) and 12 h. Dashed yellow lines highlight wound boundaries. Bars, 100 µm. (I) Quantification of wound closure over 12 h for iBMK cells. Bar graph shows mean + SEM, representing $n = 10$ wounds each for *Atg5*$^{+/+}$ and *Atg5*$^{-/-}$ pooled from four independent experiments. P-value determined using unpaired *t* test. (J) Representative immunofluorescence images of wound edge PyMT cells expressing shCTRL (top) or shATG7 (bottom) stained for endogenous paxillin to mark FAs. Cell edges outlined with dotted yellow line. Enlarged insets of boxed regions are shown. Bars, 5 µm. Insets are magnified 3.3-fold.

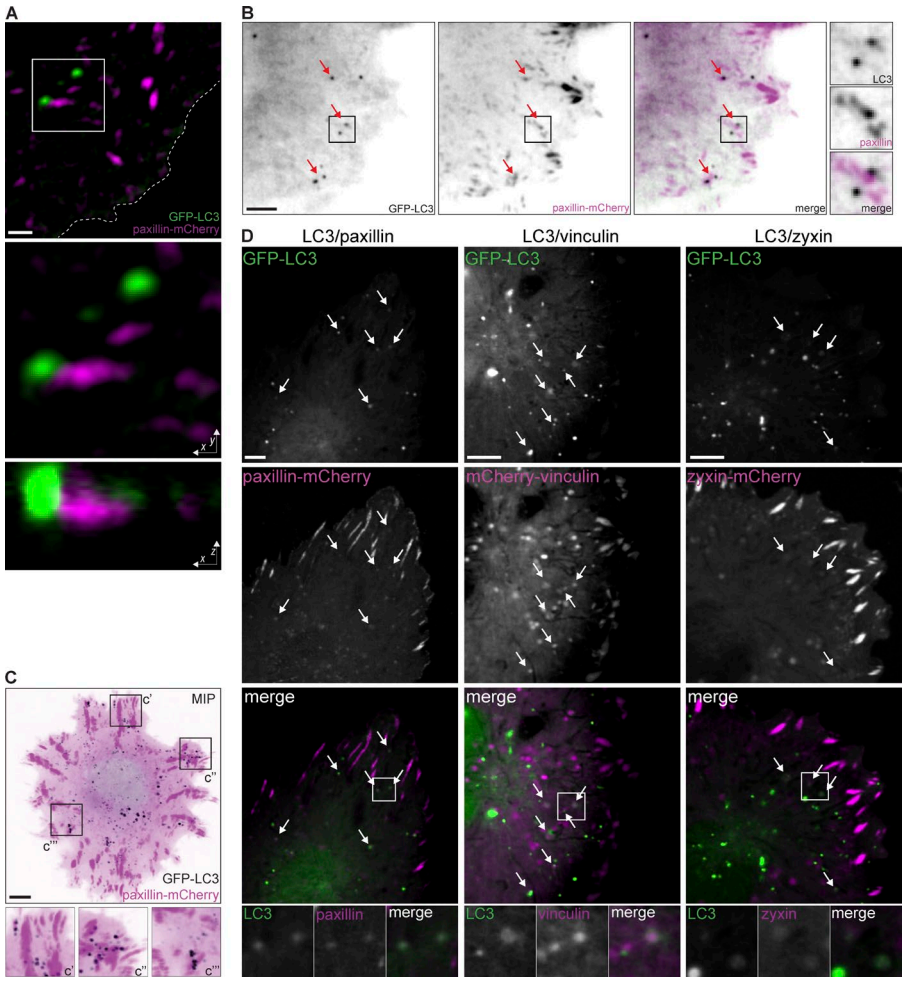

Figure S2. **Autophagosomes localize to FAs.** (A) Super-resolution SIM imaging of wound edge cells expressing GFP-LC3 to mark autophagosomes and paxillin-mCherry to mark FAs. Middle and bottom panels show x-y and x-z images of inset in boxed region, respectively. Bar, 1 µm. Insets are magnified threefold. (B) TIRF microscopy of wound edge cells expressing GFP-LC3 (black in merged image) and paxillin-mCherry (magenta in merged image). Red arrows in whole-cell images show autophagosomes localized to FAs. Right-most panel shows single-channel and merged insets of boxed region. Bar, 5 µm. Insets are magnified 2.4-fold. (C) Spinning disk confocal microscopy of a spreading cell expressing GFP-LC3 (black) and paxillin-mCherry (magenta). Top panel shows MIP of a cell over 40 min to show autophagosomes near dynamic FAs throughout the cell periphery during spreading. Boxed inset areas are shown enlarged at bottom. Bar, 5 µm. Insets are magnified 2.2-fold. (D) Spinning disk confocal microscopy of cells expressing GFP-LC3 and paxillin-mCherry (left), mCherry-vinculin (middle), or zyxin-mCherry (right). White arrows in whole-cell images indicate GFP-positive and mCherry-positive puncta. Bottom panel shows single-channel and merged insets of boxed region. Bars, 5 µm. Insets for LC3/paxillin are magnified 3.2-fold, and insets for LC3/vinculin and LC3/zyxin are magnified 2.7-fold.

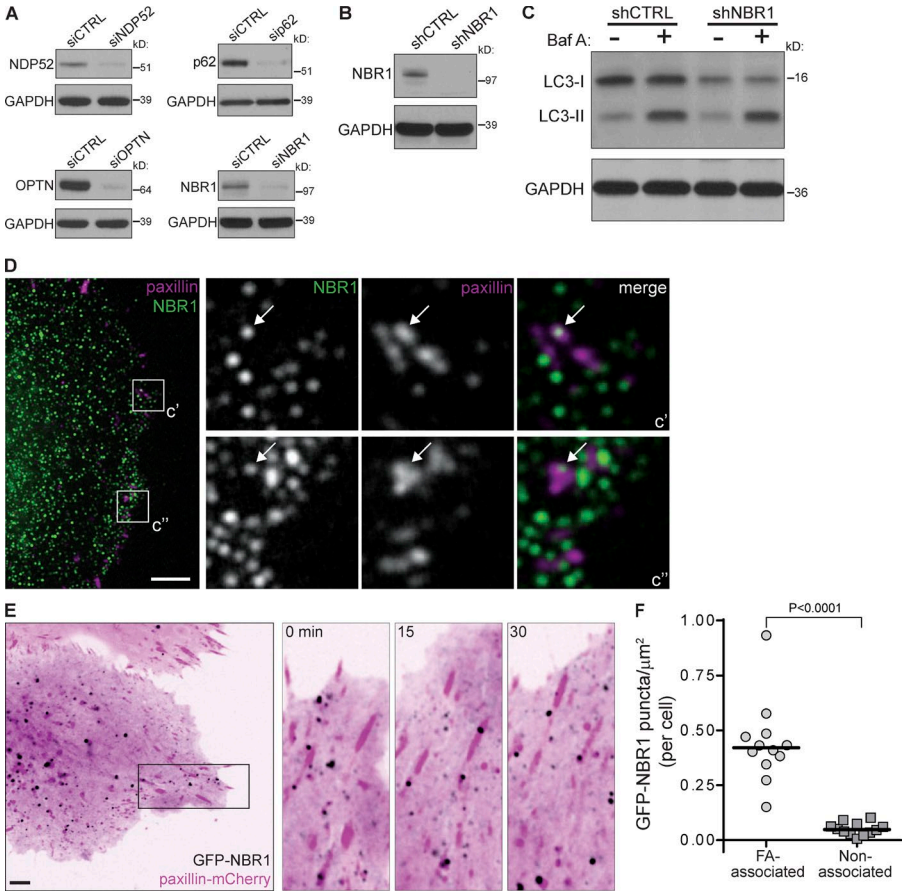

Figure S3. **Regulation of migration and FAs by the autophagy cargo receptor NBR1.** (A) siRNA-mediated depletion of the indicated autophagy cargo receptors used for scratch-wound closure assays. GAPDH is loading control. (B) shRNA knockdown of NBR1. GAPDH is loading control. (C) LC3-II turnover in the absence or presence of bafilomycin A (Baf A, 20 nM for 30 min). GAPDH is loading control. (D) Representative immunofluorescence images of wound edge cells stained for endogenous paxillin (magenta) to mark FAs and endogenous NBR1 (green). Whole-cell merged image shown at left, and enlarged boxed insets of merged and single-channel paxillin and NBR1 images shown at right. Arrow points to colocation in insets. Bar, 5 μm. Insets are magnified 4.9-fold. (E) Spinning disk confocal microscopy of a migrating cell expressing GFP-NBR1 (black) and paxillin-mCherry (magenta). Boxed region is shown as enlarged insets to the right, rotated such that the cell edge is moving upward vertically. Elapsed time (min) indicated in top left of images. Bar, 5 μm. Insets are magnified 2.4-fold. These images correspond to Video 9. (F) Analysis of GFP-NBR1 in FA areas and non-FA areas at the leading edge of migrating cells. Total GFP-NBR1 puncta at FAs or in non-FA areas was counted and normalized to the total area for FA or non-FA regions, respectively. Scatter plot shows individual single cells (n = 12 total cells) and median (line), representing 963 total leading edge GFP-NBR1 puncta analyzed from two independent experiments. P-value calculated using a nonparametric Mann-Whitney test.

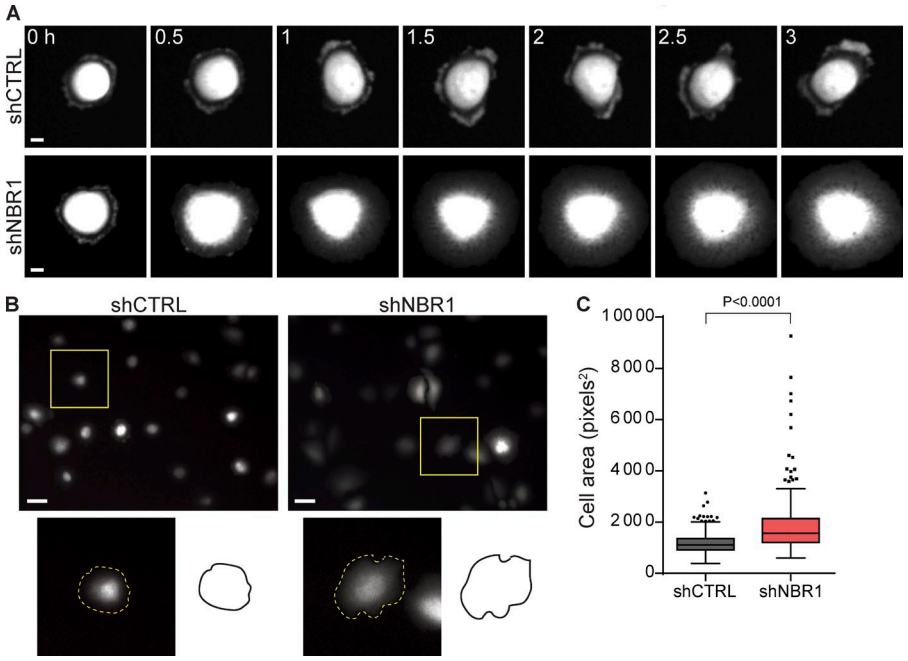

Figure S4. **NBR1 knockdown leads to enhanced cell spreading.** (A) Spinning disk confocal microscopy time-lapse sequences of cells expressing ZsGreen during spreading after replating. Representative images of shCTRL (top) and shNBR1 (bottom) cells are shown over 3 h. Elapsed time (h) indicated at top left. Bars, 10 µm. (B) Representative images of ZsGreen-labeled cells fixed at 1 h after replating. Whole-field images shown with boxed insets of individual cells enlarged at bottom left. Tracing of individual cell in inset at bottom right. Bars, 50 µm. Insets are magnified 2.4-fold. (C) Quantification of area of shCTRL- and shNBR1-expressing cells fixed 1 h after replating. Area determined by manually outlining individual ZsGreen-expressing cell borders. Data presented as median (line), first and third quartile (box), and whiskers extend to ±1.5 times the interquartile range. Individual data points outside of this range are shown. n = 211 cells for shCTRL and n = 195 cells for shNBR1, pooled from two independent experiments. These experiments were run in conjunction with two out of the three experimental repeats in Fig. 3 (B and C); therefore, quantitative data for shCTRL from those experiments are also included as part of Fig. S3 C. P-values were calculated using a nonparametric Mann-Whitney test.

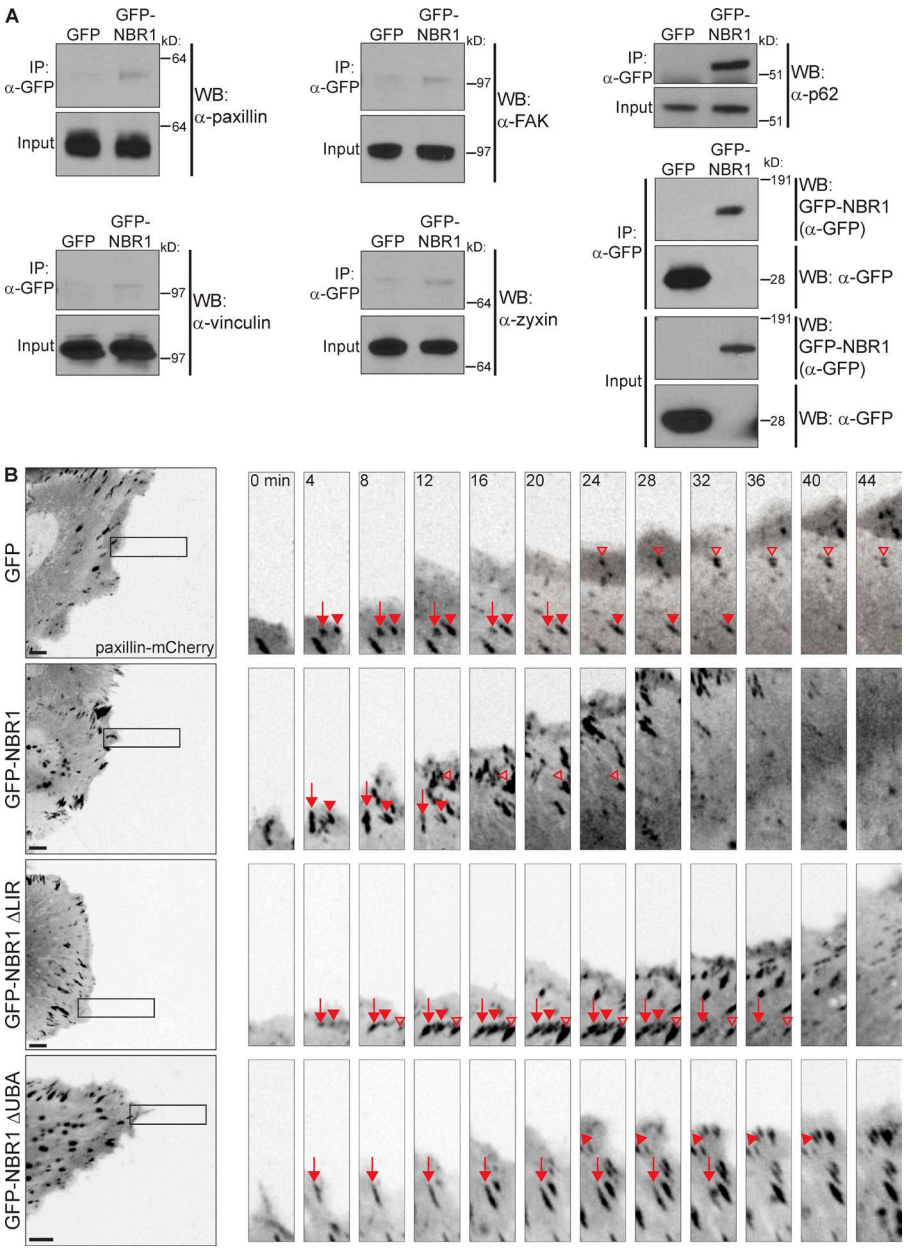

Figure S5. **NBR1 interacts with FA proteins and promotes FA disassembly.** (A) Cells stably expressing GFP or GFP-NBR1 were lysed, immunoprecipitated (IP) with anti-GFP, and immunoblotted (WB) with the indicated antibodies. (B) Spinning disk confocal microscopy time-lapse sequences of paxillin-mCherry–labeled FAs (black) in migrating cells. Left panels show representative cells expressing GFP control, GFP-NBR1, GFP-NBR1 ΔLIR, or GFP-NBR1 ΔUBA. Image sequences of boxed regions on the right have been rotated such that the cell edge with dynamic FAs is moving upward vertically. Arrows, closed arrowheads, and open arrowheads track individual FAs over time. Elapsed time (min) shown in top left of images. Bars, 5 µm. Insets are magnified 2.4-fold.

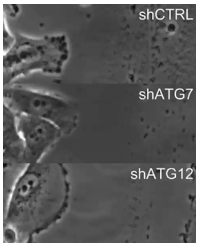

Video 1. **Single-cell tracking of migrating shCTRL-, shATG7-, and shATG12-expressing cells.** Phase-contrast microscopy of single-cell migration of shCTRL- (top), shATG7- (middle), and shATG12-expressing (bottom) cells. Images were acquired every 3 min. The video plays at 24 frames per second and is accelerated 4,320 times. This video is related to Fig. 1.

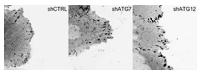

Video 2. **FA dynamics in shCTRL-, shATG7-, and shATG12-expressing cells.** Spinning disk confocal microscopy of FA turnover dynamics in shCTRL- (left), shATG7- (middle), and shATG12-expressing (right) cells. FAs are marked by paxillin-mCherry (black). Images were acquired every 2 min. The video plays at 6 frames per second and is accelerated 720 times. This video is related to Fig. 2.

Video 3. **FA dynamics at the leading edge of shCTRL-, shATG7-, and shATG12-expressing cells.** Spinning disk confocal microscopy of FA turnover dynamics at the leading edge of shCTRL- (left), shATG7- (middle), and shATG12-expressing (right) cells. These are insets from the same cells shown in Video 2. FAs are marked by paxillin-mCherry (black). Images were acquired every 2 min. The video plays at 6 frames per second and is accelerated 720 times. This video is related to Fig. 2.

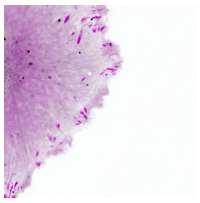

Video 4. **Migrating cell coexpressing GFP-LC3 and paxillin-mCherry.** Spinning disk confocal microscopy of a migrating cell expressing GFP-LC3 (black) to mark autophagosomes and paxillin-mCherry (magenta) to mark FAs. Images were acquired every 3 min. The video plays at 2 frames per second and is accelerated 360 times. This video is related to Fig. 4.

Video 5. **Dynamics of a nontargeted FA.** Spinning disk confocal microscopy of a leading edge nontargeted FA from a cell expressing GFP-LC3 (black) and paxillin-mCherry (magenta). This is an inset from the cell in Video 4. Images were acquired every 3 min. The video plays at 2 frames per second and is accelerated 360 times. This video is related to Fig. 4.

Video 6. **Dynamics of a GFP-LC3-targeted FA.** Spinning disk confocal microscopy of a leading edge GFP-LC3–targeted FA from a cell expressing GFP-LC3 (black) and paxillin-mCherry (magenta). This is an inset from the cell in Video 4. Images were acquired every 3 min. The video plays at 2 frames per second and is accelerated 360 times. This video is related to Fig. 4.

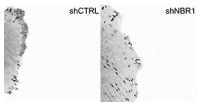

Video 7. **FA dynamics in shCTRL- and shNBR1-expressing cells.** Spinning disk confocal microscopy of FA turnover dynamics in shCTRL- (left) and shNBR1-expressing (right) cells. FAs are marked by paxillin-mCherry (black). Images were acquired every 2 min. The video plays at 6 frames per second and is accelerated 720 times. This video is related to Fig. 5.

Video 8. **FA dynamics at the leading edge of shCTRL- and shNBR1-expressing cells.** Spinning disk confocal microscopy of FA turnover dynamics at the leading edge of shCTRL- (left) and shNBR1-expressing (right) cells. These are insets from the same cells shown in Video 7. FAs are marked by paxillin-mCherry (black). Images were acquired every 2 min. The video plays at 6 frames per second and is accelerated 720 times. This video is related to Fig. 5.

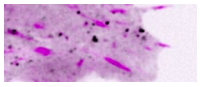

Video 9. **Migrating cell coexpressing GFP-NBR1 and paxillin-mCherry.** Spinning disk confocal microscopy of the leading edge of a migrating cell expressing GFP-NBR1 (black) and paxillin-mCherry (magenta). Images were acquired every 1.5 min. The video plays at 2 frames per second and is accelerated 180 times. This video is related to Fig. S3.